JCAMECH

Vol. 48, No. 2, 2017, pp 345-356
DOI: 10.22059/jcamech.2017.241467.184

A New Virtual Leader-Following Consensus Protocol to Stability Analysis of Longitudinal Platoon of Vehicles with Generic Network Topology under Communication and Parasitic Delays

Hossein Chehardoli[1,*], Mohammad Reza Homaeinezhad[2]

[1,2]*Department of Mechanical Engineering, K. N. Toosi University of Technology, Tehran, Iran.*

Received: 12 Sep. 2017, Accepted: 3 Nov. 2017

Abstract

In this paper, a new virtual leader following consensus protocol is introduced to perform the internal (asymptotic) stability analysis of longitudinal platoon of vehicles under generic network topology. In all previous studies on multi-agent systems with generic network topology, the control parameters are strictly dependent on eigenvalues of network matrices (adjacency or Laplacian). Since some of these eigenvalues are complex, the stability analysis with the presented methods is very hard or even impossible for large scale or time-varying networks. A new approach is introduced in this paper to decouple the large dimension closed-loop dynamics to individual third-order linear differential equations. A new spacing policy function assuring safety and increasing the traffic capacity is introduced to adjust the inter-vehicle spacing. The stable regions of communication and parasitic delays are calculated by employing the cluster treatment characteristic roots (CTCR) method. It will be shown that the presented approach assures the internal stability of large-scale platoon of vehicles with generic network topology. The most important privilege of the presented method compared with the previous approaches, is that the control gains are independent on network structure. This new finding, simplifies the stability analysis and control design specially for large scale platoons and time-varying networks. Several simulation results are provided to show the effectiveness of the proposed approaches.

Keywords:

Vehicular Platoons, Internal Stability, Generic Network Topology, Decoupling, Communication Delay, Parasitic Delay.

---

[*] Corresponding Author.
Email Address: h.chehardoli@mail.kntu.ac.ir

1. Introduction

Traffic congestion imposes an intolerable burden on urban inmates. Increasing in traffic density will cause the traffic congestion on the highways which reduce the traffic safety, increasing air pollution, traveling time, and fuel consumption [1-3]. Vehicular platooning is a useful solution for reducing the impact of traffic congestion [4, 5]. The control theory community has put much attention into developing new approaches for vehicular platoon control [6-9]. This regard is due to the important role of platoons on traffic congestion. Adaptive cruise control (ACC) is a prevalent approach for vehicular platoon control. This approach as a powerful tool in vehicular platooning has received much attention in recent decades [7, 10, 11].

For vehicular platoons, in addition to internal stability (asymptotic stability), the string stability should be investigated [12, 13]. A vehicular platoon is string stable if the spacing errors are not propagated along the group when external disturbances are applied to lead vehicle [14, 15]. The string stability analysis has been widely investigated in control design of vehicular platoons [7, 8, 12, 13, 15]. There is a direct relation between string stability and spacing policy. In general, there are two policies for spacing control of vehicular platoons: constant spacing policy (CSP) and constant time headway policy (CTHP). In CSP, the distance between successive vehicles is controlled to be constant and independent of velocity [16-18]. Whereas in CTHP, it varies linearly with velocity [19-21].

The control structure of a vehicle consists of two main parts: upper level control and lower level control [11, 12, 22]. The upper level control calculates the desired acceleration and lower level control calculates the appropriate inputs for throttle and brake actuators to produce the desired acceleration. Lower level dynamics and the vehicle itself, plays the role of node dynamics for upper level controller [10]. In a platoon, each vehicle is in communication with its neighbors and by using a suitable control law, certain objectives such as internal stability, string stability and small inter-vehicles spacing are achieved. The control design of vehicular platoons has a hierarchical structure [10]. 1) Individual vehicle dynamics, 2) Communication structure between vehicles, 3) Centralized or decentralized control scheme and 4) Inter-vehicular spacing strategy. A platoon is homogeneous if all vehicles have identical dynamics, otherwise it is called heterogeneous [10, 12].

In recent years, a large amount of research works have been accomplished on stability analysis and control design of vehicular platoons. In [22-24] several control protocols are presented assuring safety during emergency braking. Robust control against un-modeled dynamics and undesirable effects such as parameter uncertainties, data losing, and external disturbances is studied in [16] and [17]. Adaptive control is employed to estimate the parameter uncertainties such as vehicle mass, air drag force, and drag coefficient [17, 18]. Model predictive control (MPC) is considered in [14] to provide the internal and string stability of 1-D homogeneous platoons. The effect of communication time delay on performance of stability is studied in [9, 11, 12, 20, 23, 25, 26]. In [20, 23, 25] delay is assumed to be homogenous whereas in [9, 12, 22, 27] it is assumed to be heterogeneous. PDE-based approaches for formation control of vehicular platoons are investigated in [28, 29]. Second order and third order models are used to describe the longitudinal motion of platoon in [9, 19, 25, 30] and [22, 23, 28], respectively.

To the best of our knowledge, the problem of internal stability of large scale vehicular platoons with generic network topology under time delay has not been considered so far. Very few works have been carried out on small dimension platoons with generic network topology [9, 12, 22, 27, 30]. None of these approaches are robust against changing the length of platoon and usual maneuvers such as split, merge, leave, etc. In all of these studies, the length of platoon should be exactly known without any changes. In the presented methods, the control parameters are strictly dependent on eigenvalues of network matrices (adjacency or Laplacian). Therefore, the stability analysis of large scale platoons under generic communication topology with the existing methods is very hard or even impossible.

In this paper, due to large length of platoon, a new virtual leader following protocol is introduced to provide the necessary conditions on control parameters satisfying internal stability. Afterwards, by presenting a new approach, the closed-loop dynamics of platoon is decoupled to individual third-order linear differential equations. It will be shown that the proposed consensus algorithm, guarantees the stability of generic vehicular networks with finite and infinite dimensions. Due to physical considerations, both communication and parasitic delays are involved in system modeling and control design. The stable regions of delay are calculated by employing the cluster treatment characteristic roots (CTCR) method. To adjust the inter-vehicle spacing, a new spacing policy function which is the combination of CSP and CTHP is introduced.

The most important contributions of this paper are as follows: 1- introducing a new virtual leader following consensus protocol assuring internal stability of large scale vehicular networks in presence of time delay, 2- presenting a new decoupling approach which converts the infinite dimension closed-loop dynamics to individual third-order linear differential equations, 3- presenting a new spacing policy function to adjust the inter-vehicle spacing which increases safety and traffic capacity.

The rest of paper is organized as follows. In section 2, a brief review of longitudinal model of vehicle is presented. In section 3, the internal stability analysis of large-scale vehicular networks is presented. In section 4, the simulation studies are provided to show the effectiveness of the proposed methods. Finally, this paper is concluded in section 5.

2. Longitudinal Model of Platoon

Consider a group of N+1 vehicles moving in 1-D motion as shown in Fig. (1). The following differential equation describes the longitudinal motion of vehicle [10, 22, 28]

$$\dot{a}_i = h_i(v_i, a_i) + q_i(v_i) r_i \tag{1}$$

where $x_i, v_i,$ and a_i are position, velocity, and acceleration of ith vehicle, respectively and r_i is the input of engine. Also h_i and q_i are defined as follows

$$h_i(v_i, a_i) = -\frac{1}{T_i}\left(a_i + \frac{\rho H_i c_i}{2M_i} v_i^2 + \frac{R_i}{M_i}\right) - \frac{\rho H_i\, c_i v_i a_i}{M_i}$$
$$q_i(v_i) = \frac{1}{T_i\, M_i} \tag{2}$$

where ρ is the mass density of air, $T_i, H_i, c_i, R_i,$ and M_i are engine time constant, cross sectional area, air drag coefficient, rolling resistance and mass of vehicle. By taking the following lower level control

$$r_i = u_i M_i + \frac{1}{2}\rho H_i c_i v_i^2 + R_i + T_i \rho H_i c_i v_i a_i, \tag{3}$$

where u_i is the additional control input, the following third-order linear model is obtained [10, 22, 28]

$$T_i\, \dot{a}_i + a_i = u_i \tag{4}$$

The control architecture of a vehicle is composed of two levels [13]: the lower level control (r_i) which compensates the nonlinear vehicle dynamics and the upper level control (u_i) which calculates the desired acceleration of vehicle. In this paper, only upper level control is designed and it is assumed that lower level control has already been designed. Fig. (2) depicts the relationship between upper level control and lower level control.

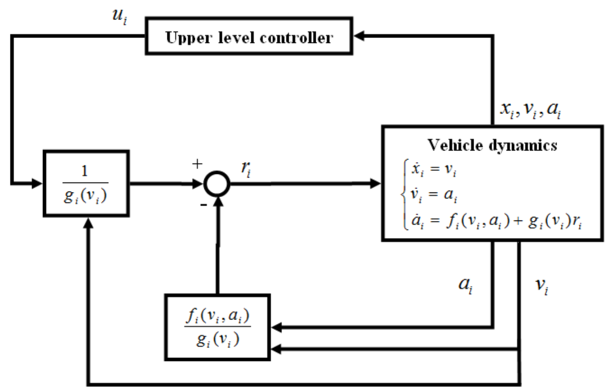

Figure 2. Relation between upper level and lower level controllers.

3. Internal Stability Analysis of Vehicular Networks with Generic Topology

In the platoon network, it is assumed that each vehicle is in communication with its neighbors through vehicle to vehicle communication (V2V) and with virtual leader through vehicle to infrastructure (V2I). The following virtual leader following scheme is considered for each vehicle

$$\begin{aligned} u_i(t) &= c_1\left(F\left(\xi_i(t)\right) - v_i(t)\right) + c_2\left(v_i(t) - v_0\right) + \\ &+ c_2\left(\frac{1}{\rho_i}\sum_{j=1}^{N_i} v_j(t-\upsilon) - v_i(t) + \frac{1}{\rho_i}\sum_{j=1}^{N_i} a_0(t-\upsilon_0)\upsilon\right) + \\ &+ c_3\left(\frac{1}{\rho_i}\sum_{j=1}^{N_i} a_j(t-\upsilon) - a_i(t)\right) \end{aligned} \tag{5}$$

where c_1, c_2, c_3 are control parameters, v_0, a_0 are velocity and acceleration of virtual leader, N_i is the number of neighbors of vehicle i, ρ_i is the in-degree of vehicle i, v_i, a_i are velocity and acceleration of each vehicle, υ, υ_0 are V2V and V2I communication delays and $\xi(t)$ is defined as follows

$$\xi_i(t) = \frac{1}{\rho_i}\sum_{k=j}^{N_i} x_k(t-\upsilon) - \sum_{k=j}^{i-1}\left(L_k + D_k\right) - x_i(t) - hv_0 +$$

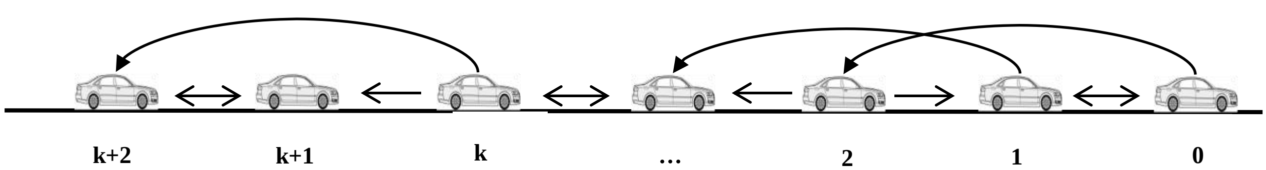

Figure 1. A 1-D homogeneous vehicular platoon with non-uniform and directed (generic) network topology

$$+\frac{1}{\rho_i}(i-j)v_0(t-\upsilon_0)\upsilon \tag{6}$$

where L_k, D_k and h are length, inter-vehicle spacing and time constant headway. Also, the spacing function $F(\xi_i(t))$ which is a combination of CSP and CTHP is defined as follows

$$F(\xi_i(t)) = \frac{v_{\max}}{2}\left(1+\tanh\left(2\pi\frac{\xi(t)-(R_1+R_2)/2}{R_2-R_1}\right)\right) \tag{7}$$

where $R_1, R_2, v_{\max}$ are positive constants. Fig. (3) shows the range policy function $F(.)$ for $R_1 = 20, R_2 = 40$ and $v_{\max} = 50$. This policy function has two main profits: 1) increasing the traffic capacity and 2) assuring safety. When $\xi_i(t) < R_1$, the lead vehicle tends to stop for safety reasons and when $\xi_i(t) > R_2$, tends to reach to maximum velocity to increase the traffic capacity.

The tracking error and its time derivative for each vehicle is defined as follows

$$e_i = x_i - v_0 t - x_i(0),\ \dot{e}_i = v_i - v_0,\ \ddot{e}_i = a_i,\ \dddot{e}_i = \dot{a}_i \tag{8}$$

By considering that $v_0 = F(\xi_{ij}(t_0))$, the control protocol (5) in terms of tracking error can be represented as follows

$$\begin{aligned} u_i(t) &= \\ &-c_1\dot{e}_i(t) + c_1F'(\xi(t_0))\left(\frac{1}{\rho_i}\sum_{j=1}^{N_i} e_j(t-\upsilon) - e_i(t)\right) + \\ &+\frac{c_2}{\rho_i}\sum_{j=1}^{N_i}\dot{e}_j(t-\upsilon) + c_3\left(\frac{1}{\rho_i}\sum_{j=1}^{N_i}\ddot{e}_j(t-\upsilon) - \ddot{e}_i(t)\right) \end{aligned} \tag{9}$$

The closed-loop dynamics of vehicle i will be in the following form by considering the parasitic delay (ζ)

$$\begin{aligned} T\dddot{e}_i + \ddot{e}_i &= \\ &c_1F'(\xi(t_0))\left(\frac{1}{\rho_i}\sum_{j=1}^{N_i} e_j(t-\bar{\upsilon}) - e_i(t-\zeta)\right) - \\ &-c_1\dot{e}_i(t-\zeta) + c_2\frac{1}{\rho_i}\sum_{j=1}^{N_i}\dot{e}_j(t-\bar{\upsilon}) + \\ &+c_3\left(\frac{1}{\rho_i}\sum_{j=1}^{N_i}\ddot{e}_j(t-\bar{\upsilon}) - \ddot{e}_i(t-\zeta)\right) \end{aligned} \tag{10}$$

By defining the error vector as $\mathbf{E} = [e_1, \dot{e}_1, \ddot{e}_1, ..., e_N, \dot{e}_N, \ddot{e}_N]$, the platoon closed-loop dynamics will be in the following form

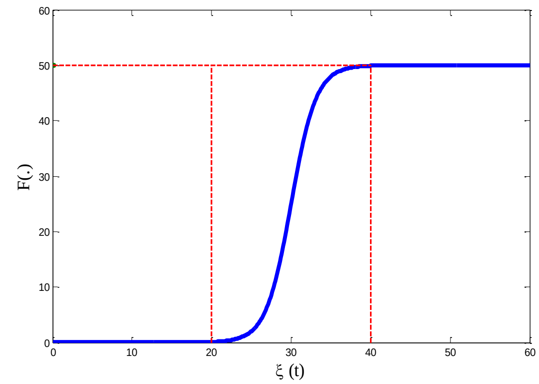

Figure 3. The range policy function F(.)

$$\begin{aligned} \dot{\mathbf{E}}(t) &= (\mathbf{I}_N \otimes \mathbf{S}_1)\mathbf{E}(t) + (\mathbf{I}_N \otimes \mathbf{S}_2)\mathbf{E}(t-\zeta) + \\ &+ (\bar{\mathbf{D}} \otimes \mathbf{S}_3)\mathbf{E}(t-\bar{\upsilon}) \end{aligned} \tag{11}$$

where $\bar{\mathbf{D}} = \mathbf{D}^{-1}\mathbf{A}$ and

$$\mathbf{S}_1 = \frac{1}{T}\begin{pmatrix} 0 & T & 0 \\ 0 & 0 & T \\ 0 & 0 & -1 \end{pmatrix},\quad \mathbf{S}_2 = -\frac{1}{T}\begin{pmatrix} 0 & 0 & 0 \\ 0 & 0 & 0 \\ c_1F'(\xi(t_0)) & c_1 & c_3 \end{pmatrix},$$

$$\mathbf{S}_3 = \frac{1}{T}\begin{pmatrix} 0 & 0 & 0 \\ 0 & 0 & 0 \\ c_1F'(\xi(t_0)) & c_2 & c_3 \end{pmatrix}$$

By applying the following theorem, the large dimension closed-loop dynamics of platoon is converted to individual third-order linear differential equations.

Theorem 1. Without loss of generality, it is assumed that the adjacency matrix **A** has n distinct real eigenvalues λ_i and m distinct complex eigenvalues $\bar{\lambda}_i = g_i + jh_i$. It is assumed that n_r and m_r are repetition orders of rth real or complex eigenvalues. Therefore, $\sum_1^n n_r + \sum_1^m m_r = N$, where N is the length of platoon. There exists a non-singular matrix $\mathbf{V} \in \Re^{N\times N}$ such that

$$\begin{aligned} &\mathbf{V}^{-1}\mathbf{A}\mathbf{V} = \mathbf{\Pi}, \\ &\mathbf{\Pi} = diag(\mathbf{\Pi}_1, ..., \mathbf{\Pi}_n, \mathbf{\Pi}_{n+1}, ..., \mathbf{\Pi}_{n+m}) \end{aligned} \tag{12}$$

where $\mathbf{\Pi}_i, i = 1,2,...,n$ are Jordan blocks associated to real eigenvalues. For repetitive real eigenvalues, these blocks are in the following form

$$\mathbf{\Pi}_i = \begin{bmatrix} \lambda_i & 1 & \cdots & 0 \\ 0 & \lambda_i & \ddots & \vdots \\ \vdots & \ddots & \ddots & \underline{\nu} \\ 0 & \cdots & 0 & \lambda_i \end{bmatrix} \tag{13}$$

Based on nilpotent matrices associated to $\lambda_i, \underline{\nu} \in \{0,1\}$, [31]. Moreover, Jordan blocks associated to $\bar{\lambda}_i$ are as follows $(i = n+1,...,n+m)$

$$\mathbf{\Pi}_i = \begin{bmatrix} \bar{\mathbf{\Pi}}_i & \mathbf{I}_2 & & \\ 0 & \bar{\mathbf{\Pi}}_i & \ddots & \\ \vdots & \ddots & \ddots & \mathbf{I}_2 \\ 0 & ... & 0 & \bar{\mathbf{\Pi}}_i \end{bmatrix}, \bar{\mathbf{\Pi}}_i = \begin{bmatrix} g_i & h_i \\ -h_i & g_i \end{bmatrix} \tag{14}$$

Proof. Appendix 1.

According to theorem 1, there exists a non-singular matrix $\mathbf{V}$ such that, $\mathbf{V}^{-1}\mathbf{A}\mathbf{V} = \mathbf{\Pi}$, where $\mathbf{\Pi}$ is the Jordan canonical form of matrix $\mathbf{A}$. By defining $\mathbf{E} = (\mathbf{V} \otimes \mathbf{I}_3)\bar{\mathbf{E}}$, (11) can be written in the following form:

$$\begin{aligned} \dot{\bar{\mathbf{E}}} &= (\mathbf{V}^{-1} \otimes \mathbf{I}_3)(\mathbf{I}_N \otimes \mathbf{S}_1)(\mathbf{V} \otimes \mathbf{I}_3)\bar{\mathbf{E}}(t) + \\ &+ (\mathbf{V}^{-1} \otimes \mathbf{I}_3)(\mathbf{I}_N \otimes \mathbf{S}_2)(\mathbf{V} \otimes \mathbf{I}_3)\bar{\mathbf{E}}(t-\zeta) + \\ &+ (\mathbf{V}^{-1} \otimes \mathbf{I}_3)(\bar{\mathbf{D}} \otimes \mathbf{S}_3)(\mathbf{V} \otimes \mathbf{I}_3)\bar{\mathbf{E}}(t-\bar{\upsilon}) \end{aligned} \tag{15}$$

By applying lemma (1) to (15), we will have

$$\begin{aligned} \dot{\bar{\mathbf{E}}} &= (\mathbf{I}_N \otimes \mathbf{S}_1)\bar{\mathbf{E}}(t) + (\mathbf{I}_N \otimes \mathbf{S}_2)\bar{\mathbf{E}}(t-\zeta) + \\ &+ (\mathbf{\Pi} \otimes \mathbf{S}_3)\bar{\mathbf{E}}(t-\bar{\upsilon}) \end{aligned} \tag{16}$$

Theorem 2. Under the following conditions and sufficiently small time delay, system (16) is globally asymptotically stable.

$$\begin{aligned} & c_1 \geq c_2, \\ & c_3 \geq \max\left\{ \frac{c_1}{c_1 - c_2} TF'(\xi(t_0)), TF'(\xi(t_0)) - 1 \right\} \\ & \mathbf{L}_1 = \frac{\mathbf{L}_2^T \mathbf{P}^{-1}}{2} \end{aligned} \tag{17}$$

where $\mathbf{L}_1 = [c_1 F'(\xi(t_0)), c_2, c_3]$, $\mathbf{L}_2 = [0, 0, 1/T]^T$ and $\mathbf{P}$ is a positive definite matrix satisfying $(\mathbf{S}_1 + \mathbf{S}_2)\mathbf{P} + \mathbf{P}(\mathbf{S}_1^T + \mathbf{S}_2^T) \prec \mathbf{0}$.

Proof. System (16) without time delay should be stable. The matrix $\mathbf{I}_N \otimes \mathbf{S}_1 + \mathbf{I}_N \otimes \mathbf{S}_2 + \mathbf{\Pi} \otimes \mathbf{S}_3$ is in fact a block upper diagonal matrix. For real eigenvalues, these blocks will be in the following form

$$\begin{bmatrix} \mathbf{\Theta}_i & \mathbf{S}_3 & & \\ & \mathbf{\Theta}_i & \ddots & \\ & \ddots & \ddots & \underline{\nu}\mathbf{S}_3 \\ & & & \mathbf{\Theta}_i \end{bmatrix}, \begin{cases} \mathbf{\Theta}_i = \mathbf{S}_1 + \mathbf{S}_2 + \lambda_i \mathbf{S}_3 \\ \lambda_i \in \Re, \qquad i = 1,...,n \end{cases} \tag{18}$$

and for complex eigenvalues in the following form

$$\begin{bmatrix} \bar{\mathbf{\Theta}}_i & \mathbf{I}_2 \otimes \mathbf{S}_3 & & \\ & \bar{\mathbf{\Theta}}_i & \ddots & \\ & \ddots & \ddots & \mathbf{I}_2 \otimes \mathbf{S}_3 \\ & & & \bar{\mathbf{\Theta}}_i \end{bmatrix}, i = n+1,...,n+m,$$

$$\begin{cases} \bar{\mathbf{\Theta}}_i = \mathbf{I}_2 \otimes (\mathbf{S}_1 + \mathbf{S}_2) - \begin{pmatrix} g_i & h_i \\ -h_i & g_i \end{pmatrix} \otimes \mathbf{S}_3 \\ \bar{\lambda}_i = g_i + jh_i \end{cases} \tag{19}$$

According to matrix theory [31], system (13) without delay is asymptotically stable if $\bar{\mathbf{\Theta}}_i, \mathbf{\Theta}_i \prec \mathbf{0}$. The characteristic equation of $\mathbf{\Theta}_i$ is as follows

$$\begin{aligned} & Ts^3 + \left[(1-\lambda_i)c_3 + 1\right]s^2 + (c_1 - c_2\lambda_i)s + \\ & + c_1 F'(\xi(t_0))(1-\lambda_i) = 0 \end{aligned} \tag{20}$$

By employing the Routh-Hurwitz criterion, it can be found that under the following conditions, (20) is asymptotically stable

$$\begin{aligned} & c_1 F'(\xi(t_0))(1-\lambda_i) > 0, \quad (1-\lambda_i)(c_1 - c_2\lambda_i)c_3 + \\ & \quad + (c_1 - c_2\lambda_i) - c_1 T(1-\lambda_i)F'(\xi(t_0)) > 0 \end{aligned} \tag{21}$$

According to Gersgorin theorem (appendix 2), $|\lambda_i| < 1$. Therefore, (1-21) is always satisfied. It can be verified that under condition (1-17), (2-21) is satisfied.

In continuance of proof, from lemma (2), it is inferred that system (19) is asymptotically stable if there exists a positive definite matrix $\mathbf{P}$ satisfying the following inequality

$$\begin{aligned} & \left(\mathbf{I}_2 \otimes (\mathbf{S}_1 + \mathbf{S}_2) - \begin{pmatrix} g_i & h_i \\ -h_i & g_i \end{pmatrix} \otimes \mathbf{S}_3\right)(\mathbf{I}_2 \otimes \mathbf{P}) + \\ & + (\mathbf{I}_2 \otimes \mathbf{P})\left(\mathbf{I}_2 \otimes (\mathbf{S}_1^T + \mathbf{S}_2^T) - \begin{pmatrix} g_i & -h_i \\ h_i & g_i \end{pmatrix} \otimes \mathbf{S}_3^T\right) \prec \mathbf{0} \end{aligned} \tag{22}$$

Since $\mathbf{S}_3 = \mathbf{L}_2\mathbf{L}_1$, by choosing $\mathbf{L}_1 = \mathbf{L}_2^T\mathbf{P}^{-1}/2$ and doing some simplifications, we will have

$$\begin{aligned} & \mathbf{I}_2 \otimes \left((\mathbf{S}_1 + \mathbf{S}_2)\mathbf{P} + \mathbf{P}(\mathbf{S}_1^T + \mathbf{S}_2^T)\right) - \\ & - \begin{pmatrix} g_i & 0 \\ 0 & g_i \end{pmatrix} \otimes (\mathbf{L}_2\mathbf{L}_2^T) \prec \mathbf{0} \end{aligned} \tag{23}$$

Since $-\begin{pmatrix} g_i & 0 \\ 0 & g_i \end{pmatrix} \otimes (\mathbf{L}_2\mathbf{L}_2^T)$ is a negative semi-definite matrix, therefore eq. (23) is always negative definite. By calculating the stable regions of time delay, the proof will be complete. In continuance, a brief review of D-subdivision method is presented. By employing (18) and

(19), the characteristic equations of (16) for real and complex eigenvalues are as eqs. (24) and (25), respectively.

$$\begin{aligned} ce_i &= \det\left(s\mathbf{I}_3 - \mathbf{S}_1 - \mathbf{S}_2 e^{-\varsigma s} - \lambda_i \mathbf{S}_3 e^{-\bar{\nu} s}\right) = \\ &= Ts^3 + s^2 + c_3\left(e^{-\zeta s} - \lambda_i e^{-\bar{\nu} s}\right)s^2 + \\ &+\left(c_1 e^{-\varsigma s} - c_2\lambda_i e^{-\bar{\nu} s}\right)s + c_1 F'\left(\xi_{ij}(0)\right)\left(e^{-\zeta s} - \lambda_i e^{-\bar{\nu} s}\right) \end{aligned} \quad (24)$$

$$\overline{ce_i} = \det \left(s\mathbf{I}_6 - \mathbf{I}_2 \otimes \mathbf{S}_1 - \begin{pmatrix} g & h \\ -g & h \end{pmatrix} \otimes \mathbf{S}_2 e^{-\zeta s} - \mathbf{I}_2 \otimes \mathbf{S}_3 e^{-\bar{\nu} s}\right) \quad (25)$$

Since ce_i and $\overline{ce_i}$ have infinite roots, the stability analysis of (24) and (25) by using Routh-Hurwitz is really hard or impossible. Therefore, the following Rekasius transformations are applied to achieve a finite dimension polynomial [32].

$$e^{-\bar{\nu} s} = \frac{1-\bar{T}_1 s}{1+\bar{T}_1 s}, \quad e^{-\zeta s} = \frac{1-\bar{T}_2 s}{1+\bar{T}_2 s}, \quad s = j\omega,\ \omega \in \Re^+ \quad (26)$$

Under the Rekasius transformation, all imaginary roots of eqs. (24) and (25) remain invariant [32]. By considering $s = j\omega$, defining $v_1 = \bar{T}_1\omega$, $v_2 = \bar{T}_2\omega$ and replacing (26) in (25) and (24), we obtain that

$$\begin{aligned} ce_i &= \sum_{k=0}^{5} y_k(T, c_i, \bar{\nu}, \zeta, g, h)\omega^k + \\ &+ j\sum_{k=0}^{5} z_k(T, c_i, \bar{\nu}, \zeta, g, h)\omega^k = 0 \\ \overline{ce_i} &= \sum_{k=0}^{8} \bar{y}_k(T, c_i, \bar{\nu}, \zeta, g, h)\omega^k + \\ &+ j\sum_{k=0}^{8} \bar{z}_k(T, c_i, \bar{\nu}, \zeta, g, h)\omega^k = 0 \end{aligned} \quad (27)$$

If there is a solution $\omega \in \Re^+$ for eqs. (24) and (25), both their real and imaginary parts must be zero simultaneously. If the Sylvester's matrices associated to eq. (27) are singular, there exit imaginary roots for eqs. (24) and (25). The Sylvester's matrix associated to eq. (1-27) is in the following form

$$\mathbf{M} = \begin{pmatrix} y_3 & y_2 & y_1 & y_0 & 0 & 0 \\ 0 & y_3 & y_2 & y_1 & y_0 & 0 \\ 0 & 0 & y_3 & y_2 & y_1 & y_0 \\ z_3 & z_2 & z_1 & z_0 & 0 & 0 \\ 0 & z_3 & z_2 & z_1 & z_0 & 0 \\ 0 & 0 & z_3 & z_2 & z_1 & z_0 \end{pmatrix}$$

We can express that

$$\det(\mathbf{M}) = J(v_1, v_2) = J\left(\tan(0.5\zeta\omega), \tan(0.5\bar{\nu}\omega)\right) \quad (28)$$

which constitutes a closed-form description of the kernel curves in the spectral delay space (SDS) $(\zeta\omega, \bar{\nu}\omega)$ [32]. Every point $(\zeta\omega, \bar{\nu}\omega)$ on SDS brings an imaginary characteristic root at $\pm j\omega$. By using the transformation $(\nu, \zeta) = 2\left(\tan^{-1}(v_1, v_2) \pm k\pi\right)/\omega,\ k = 0,1,2,...$, the kernel and offspring hypercurves are derived from SDS [32]. For an imaginary root $s = j\omega$, the root tendency is defined as follows [32]

$$RT\Big|_{s=j\omega}^{\tau_j} = \operatorname{sgn}\left[\operatorname{Re}\left(\frac{\partial s}{\partial \tau}\bigg|_{s=j\omega}\right)\right] \quad (29)$$

If the root tendency is positive, by increasing the amount of delay, the imaginary root $s = j\omega$ will move to right side of imaginary axis. By using kernel and offspring hypercurves and concept of root tendency, the stable regions of time delay for characteristic equations (24) and (25) are obtained. For more details about D-subdivision method, readers are referred to [32].

Remark. The internal stability analysis of large scale heterogeneous vehicular platoons is another important issue which will be considered later.

4. Simulation Study

In this section, a platoon of ten vehicles is considered according to Fig. (4). Table (1) shows the control and system parameters used in simulation studies.

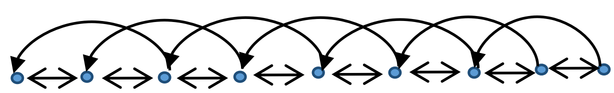

Figure 4. Communication topology of platoon.

Table 1. Control gains and system parameters

$c_1 = 4.51$	$c_2 = 1.92$	$c_3 = 2.37$	$T = 0.1s$
$R_1 = 8m$	$R_2 = 15m$	$\zeta = 0.1s$	$\nu = 0.12s$

The eigenvalues of adjacency matrix are equal to -1.36 $\pm$ j0.84,-1.18 $\pm$ j0.49,-1,-0.32,2.46,2.02,0.55,1.36. In the simulation studies, the constant time headway is considered as h=0.85s. Fig. (5) depicts the SDS diagrams for eigenvalues of adjacency matrix. By employing SDS diagram, the kernel (red curves) and offspring (blue curves) hypercurves are obtained according to Fig. (6). This figure shows the stable region of communication and parasitic delays. In all simulation results, the spacing error is defined as $\delta_i = x_{i-1} - \bar{x}_i - L - hv_0$. Figs. (7) and (8) show the spacing error and velocity of platoon for point "a". According to these figures, point "a" depicts a stable behavior for vehicles motion. Fig. (9) shows the unstable behavior of platoon for point “b”. As it is expected from Fig. (6), for this point, the platoon behavior is internal unstable. To study the effect of external disturbance applying to lead vehcile on internal and string stability, the disturbance signal $d(t)=2.47\sin(0.1\pi t)$ in time period $t\in[60,120]$ is applied to lead vehicle. According to Fig. (10), the platoon is string stable in presence of external disturbance.

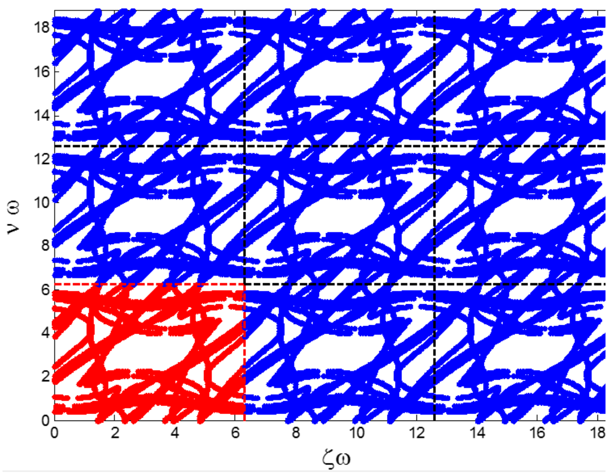

Figure 5. Spectral delay space for eigenvalues of adjacency matrix

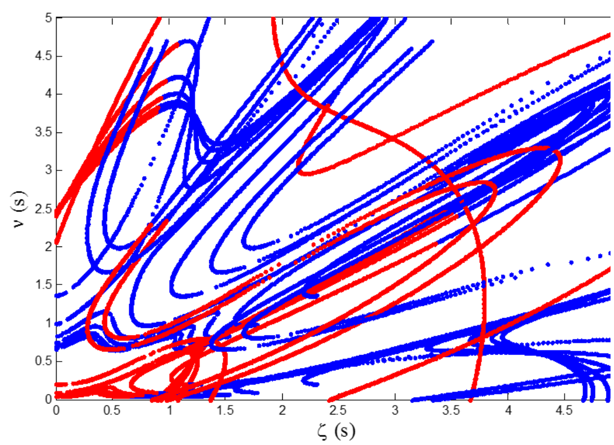

Figure 6 (a). Kernel and ospring hypercurves

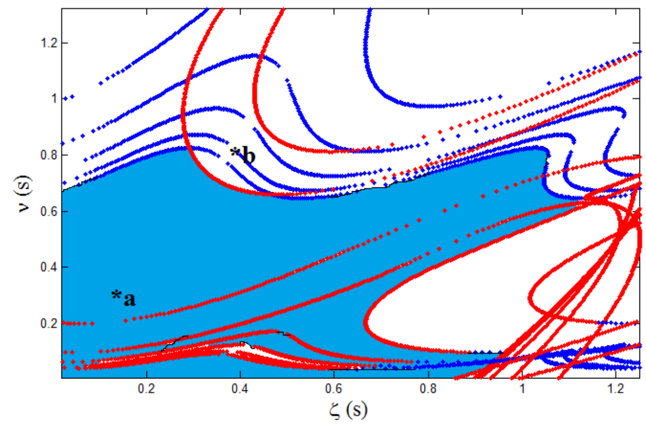

Figure 6 (b). Stable and u stable regions for communication and parasitic delays

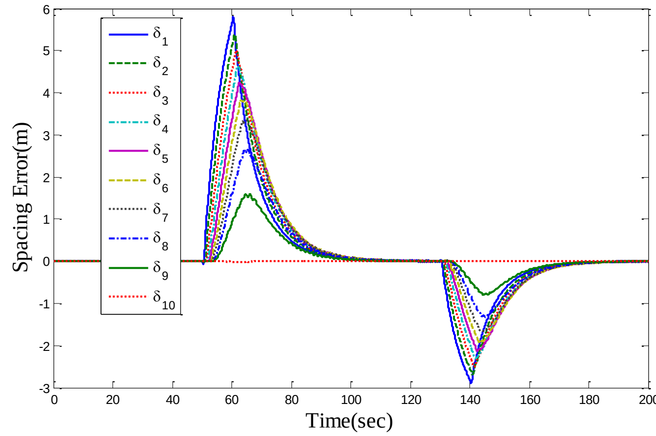

Figure 7. Spacing error of platoon, point “a”

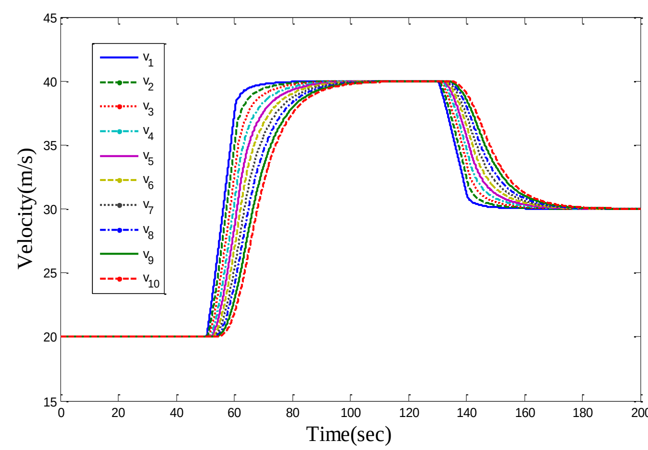

Figure 8. Velocity of platoon, point “a”

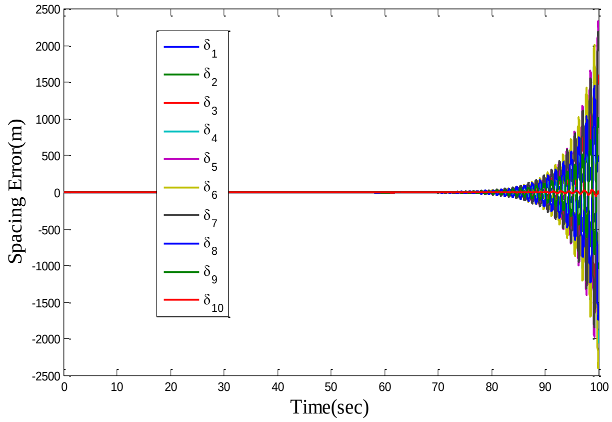

Figure 9. Unstable behaviour of platoon, point "b"

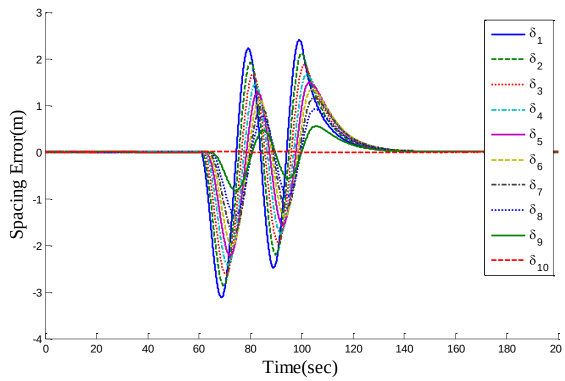

Figure 10. Internal and string stable behaviour in presence of external disturbance, point "a"

5. Conclusion

This paper presented a new approach to stability analysis and control design of vehicular platoons with large dimension. Due to large length of platoon, a new virtual leader following consensus protocol was proposed in this paper. By presenting a new decoupling approach, the large scale closed-loop dynamics was transformed to individual third-order linear dynamics. A new spacing policy was proposed to adjust the inter-vehicle spacing. Both parasitic and communication delays were considered in system modeling and stability analysis. The D-subdivision method was employed to calculate the stable regions of delays. The most important results of this paper are decoupling the large scale dimension closed-loop dynamics based on a new headway policy and the independency of control parameters on network structure. Several simulation results were provided to show the effectiveness of the proposed methods.

6. References

[1] Y. Li, D. Sun, W. Liu, M. Zhang, M. Zhao, X. Liao, L. Tang, Modeling and simulation for microscopic traffic flow based on multiple headway, velocity and acceleration difference, *Nonlinear Dynamics,* Vol. 66, No. 1, pp. 15-28, 2011.

[2] F. Y. Wang, Parallel control and management for intelligent transportation systems: Concepts, architectures, and applications, *IEEE Transactions on Intelligent Transportation Systems,*Vol. 11, No. 3, pp. 630-638, 2010.

[3] H. Ge, R. Cheng, L. Lei, The theoretical analysis of the lattice hydrodynamic models for traffic flow theory, *Physica A: Statistical Mechanics and its Applications,* Vol. 389, No. 14, pp. 2825-2834, 2010.

[4] F. Wang, K. Wang, W. Lin, X. Xu, C. Chen, Data-driven intelligent transportation systems: A survey, *IEEE Transaction on Intelligent Transpprtation System,* Vol. 12, No. 4, pp. 1624-1639, 2011.

[5] D. Jia, D. Ngoduy, Platoon based cooperative driving model with consideration of realistic inter-vehicle communication, *Transportation Research Part C: Emerging Technology,* Vol. 68, pp. 245-264, 2016.

[6] M. Amoozadeh, H. Deng, C. N. Chuah, H. M. Zhang, D. Ghosal, Platoon management with cooperative adaptive cruise control enabled by VANET, *Vehicular Communication,* Vol. 13, pp. 110-123, 2015.

[7] K. Santhana, R. Rajamani, On spacing policies for highway vehicle automation, *IEEE Transaction Intelligent Transportation System,* Vol. 4, No. 4, pp. 147-155, 2003.

[8] A. Ghasemi, R. Kazemi, S. Azadi, Stable decentralized control of platoon of vehicles with heterogeneous information feedback, *IEEE Transaction Vehicular Technology,* Vol. 62, pp. 4299–4308, 2013.

[9] M. Bernardo, A. Salvi, S. Santini, Distributed consensus Strategy for platooning of vehicles in the presence of time-varying heterogeneous communication delays, *IEEE Transaction Inelligent Transportation System,* Vol. 16, No. 1, pp. 102-112, 2015.

[10] R. Rajamani, 2011, *Vehicle dynamics and control*, Springer Science & Business Media,

[11] G. J. Naus, R. P. Vugts, J. Ploeg, M. J. van de Molengraft, M. Steinbuch, String-stable CACC design and experimental validation: A frequency-domain approach, *IEEE Transactions on vehicular technology,* Vol. 59, No. 9, pp. 4268-4279, 2010.

[12] H. Chehardoli, M. R. Homaeinezhad, Stable control of a heterogeneous platoon of vehicles with switched interaction topology, time-varying communication delay and lag of actuator, *Proc. Inst. Mechanical Engin., Part C: J. Mech. Engin. Sci.*, Vol. 231, No. 22, pp. 4197-4208.

[13] M. E. Khatir, E. Davidson, Bounded stability and eventual string stability of a large platoon of vehicles using non-identical controllers, in *Proceeding of,* IEEE, pp. 1111-1116, 2015.

[14] R. Kianfar, P. Falcone, J. Fredriksson, A control matching model predictive control approach to string stable vehicle platooning, *Control Engineering Practice,* Vol. 45, pp. 163-173, 2015.

[15] R. H. Middleton, J. H. Braslavsky, String instability in classes of linear time invariant formation control with limited communication range, *IEEE Transactions on Automatic Control*, Vol. 55, No. 7, pp. 1519-1530, 2010.

[16] X. Guo, J. Wang, F. Liao, R. S. H. Teo, Distributed adaptive integrated-sliding-mode controller synthesis for string stability of vehicle platoons, *IEEE Transactions on Intelligent Transportation Systems,* Vol. 17, No. 9, pp. 2419-2429, 2016.

[17] D. Swaroop, J. K. Hedrick, S. B. Choi, Direct adaptive longitudinal control of vehicle platoons, *IEEE Transactions on Vehicular Technology,* Vol. 50, No. 1, pp. 150-161, 2001.

[18] H. Chehardoli, M. R. Homaeinezhad, A. Ghasemi, Adaptive Centralized/Decentralized Control and Identification of 1-D Heterogeneous Vehicular Platoons Based on Constant Time Headway Policy, *IEEE Transactions on Intelligent Transportation Systems,* pp. 1-11, 2017, DOI: 10.1109/TITS.2017.2781152.

[19] H. Chehardoli, M. R. Homaienezhad, Switching decentralized control of a platoon of vehicles with time-varying heterogeneous delay: a safe and dense spacing policy, J. Automobile Eng., pp. 1-13, 2017, DOI: 10.1177/0954407017725448.

[20] A. Ghasemi, R. Kazemi, S. Azadi, Exact stability of a platoon of vehicles by considering time delay and lag, *Journal of Mechanical Science and Technology,* Vol. 29, No. 2, pp. 799, 2015.

[21] C. Wang, H. Nijmeijer, String stable heterogeneous vehicle platoon using cooperative adaptive cruise control, in *Proceeding of,* IEEE, pp. 1977-1982, 2015.

[22] H. Chehardoli, M. R. Homaienezhad, Third order safe consensus of heterogeneous vehicular platoons with MPF topology: constant time headway strategy, *J. Automobile Eng.,* pp. 1-13, 2017, DOI: 10.1177/0954407017729309.

[23] A. Ghasemi, S. Rouhi, A safe stable directional vehicular platoon, *Proceedings of the Institution of Mechanical Engineers, Part D: Journal of Automobile Engineering,* Vol. 229, No. 8, pp. 1083-1093, 2015.

[24] L. Xu, L. Y. Wang, G. Yin, H. Zhang, Communication information structures and contents for enhanced safety of highway vehicle platoons, *IEEE Transactions on vehicular Technology,* Vol. 63, No. 9, pp. 4206-4220, 2014.

[25] A. A. Peters, R. H. Middleton, O. Mason, Leader tracking in homogeneous vehicle platoons with broadcast delays, *Automatica,* Vol. 50, No. 1, pp. 64-74, 2014.

[26] L. Zhang, G. Orosz, Motif-based design for connected vehicle systems in presence of heterogeneous connectivity structures and time delays, *IEEE Transactions on Intelligent Transportation Systems,* Vol. 17, No. 6, pp. 1638-1651, 2016.

[27] A. Salvi, S. Santini, A. S. Valente, Design, analysis and performance evaluation of a third order distributed protocol for platooning in the presence of time-varying delays and switching topologies, *Transportation Research Part C: Emerging Technologies,* Vol. 80, pp. 360-383, 2017.

[28] A. Ghasemi, R. Kazemi, S. Azadi, Stable decentralized control of a platoon of vehicles with heterogeneous information feedback, *IEEE Transactions on Vehicular Technology,* Vol. 62, No. 9, pp. 4299-4308, 2013.

[29] H. Chehardoli, M. R. Homaeinezhad, Third-order leader-following consensus protocol of traffic flow formed by cooperative vehicular platoons by considering time delay: constant spacing strategy, *Proc. Inst. Mech. Eng., Part I:*

J. System and Control Engineering, pp. 1-14, 2017, DOI:10.1177/0959651817750521.

[30] H. Chehardoli, M.R. Homaeinezhad, Control of a heterogeneous platoon of vehicles with actuator lag, communication delay and switched interaction topology: constant spacing and constant time headway policy, *J. Control*, Vol. 11, No. 1, pp. 27-37, 2017.

[31] C. D. Meyer, 2000, *Matrix analysis and applied linear algebra*, Siam,

[32] A. F. Ergenc, N. Olgac, H. Fazelinia, Extended Kronecker summation for cluster treatment of LTI systems with multiple delays, *SIAM Journal on Control and Optimization*, Vol. 46, No. 1, pp. 143-155, 2007.

7. Appendix

7.1. Graph theory

Let $G=(V,E,\mathbf{A})$ is a graph of order N with $V=\{1,2,...,N\}$ which represents node set, $E\subseteq N\times N$ is the set of edges and $\mathbf{A}$ is the adjacency matrix with non-negative elements. An edge (i,j) denotes that the node j has access to the information of the node i. Set of neighbors of node i is shown by $N_i=\{j\in V:(j,i)\in\varepsilon, j\neq i\}$. The diagonal in-degree matrix of a network is $\mathbf{D}=[D_{ij}]\in\Re^{n\times n}$, with $D_{jj}=\rho_j=\sum_{k=1}^{n}a_{jk}$ and $D_{jj}=0$, for $j\neq k$. In the leader-follower scheme, for the follower agents 1 to N, there exists a leader labeled by 0. Information is exchanged between the leader and the follower agents which belong to the neighbors of the leader. Then, the graph $\bar{G}=(\bar{V},\bar{E},\mathbf{A})$ with node set $\bar{V}=V\cup\{0\}$ and edge set $\bar{E}=\bar{V}\times\bar{V}$ represents the communication topology between the leader and the followers. A diagonal matrix $\mathbf{B}\in\Re^{N\times N}$ is defined as a leader adjacency matrix of $\bar{G}$ with diagonal elements $b_i=a_{i0}$. If lead vehicle is a neighbor of vehicle i, $a_{i0}>0$ and $a_{i0}=0$, otherwise. Node 0 is globally reachable in $\bar{G}$ if there is a path form every node $i\in V$ to it. For graph G the Laplacian matrix $\mathbf{L}=[l_{ij}]\in\Re^{N\times N}$ is defined with $l_{ii}=\sum_{j=1,\neq i}^{N}a_{ij}$ and $l_{ij}=-a_{ij}, i\neq j$. Also, for graph $\bar{G}$ the important matrix $\mathbf{H}=\mathbf{L}+\mathbf{B}$ is defined.

7.2. Mathematical lemmas

Lemma 1. [31]: An arbitrary matrix $\mathbf{\Lambda}$ is asymptotically stable if there exists a positive definite matrix $\mathbf{P}$ satisfying $\mathbf{\Lambda P}+\mathbf{P\Lambda}^T\succ\mathbf{0}$.

Lemma 2. [31]: The sum of two definite and semi-definite matrices is a definite matrix.

Lemma 3. [31]: For arbitrary matrices $\mathbf{X},\mathbf{H},\mathbf{K},\mathbf{\Sigma}$ with appropriate dimension, we have $(\mathbf{X}\otimes\mathbf{H})(\mathbf{K}\otimes\mathbf{\Sigma})=(\mathbf{XK})\otimes(\mathbf{H\Sigma})$.

7.3. Proof of theorem 1

A non-singular matrix $\tilde{\mathbf{V}}$ can be found such that

$$\tilde{\mathbf{V}}^{-1}\mathbf{\Psi}\tilde{\mathbf{V}}=\tilde{\mathbf{\Pi}},$$
$$\tilde{\mathbf{\Pi}}=diag\{\tilde{\mathbf{\Pi}}_1,...,\tilde{\mathbf{\Pi}}_n,\tilde{\mathbf{\Pi}}_{n+1},\tilde{\mathbf{\Pi}}_{n+1}^*,...,\tilde{\mathbf{\Pi}}_{n+m},\tilde{\mathbf{\Pi}}_{n+m}^*\} \quad \text{(A1)}$$

where $\tilde{\mathbf{\Pi}}_i, i=1,...,n$, are in the form (13), $\tilde{\mathbf{\Pi}}_i$, $i=n+1,...,n+m$, are in the form of (14) and $(*)$ denotes the complex conjugate operator. Also, $\tilde{\mathbf{V}}$ is in the following form

$$\tilde{\mathbf{V}}=\left(\tilde{\mathbf{V}}_1,\tilde{\mathbf{V}}_2,...,\tilde{\mathbf{V}}_{n+m}\right) \quad \text{(A2)}$$

For real eigenvalues, $\tilde{\mathbf{V}}_i\in\Re^{N\times n_i}, i=1,2,...,n$ and for complex eigenvalues, $\tilde{\mathbf{V}}_i\in\Re^{N\times m_i}, i=n+1,...,n+m.$ For $n+1\leq r\leq n+m$, we have

$$\mathbf{\Psi}\tilde{\mathbf{V}}_r=\tilde{\mathbf{V}}_r\tilde{\mathbf{\Pi}}_r,\quad \mathbf{\Psi}\tilde{\mathbf{V}}_r^*=\tilde{\mathbf{V}}_r^*\tilde{\mathbf{\Pi}}_r^* \quad \text{(A3)}$$

$\tilde{\mathbf{V}}_r$ can be expressed as $\tilde{\mathbf{V}}_r=\left(\mathbf{v}_{r1},\mathbf{v}_{r2},...,\mathbf{v}_{rn_r}\right)$. $\mathbf{v}_{rk}$ can be defined as

$$\mathbf{v}_{rk}=\bar{\mathbf{v}}_{rk}+j\tilde{\mathbf{v}}_{rk},\quad 1\leq k\leq n_r;\ \bar{\mathbf{v}}_{rk},\tilde{\mathbf{v}}_{rk}\in\Re^N \quad \text{(A4)}$$

By using (A3) for k=1, we have

$$\mathbf{\Psi}\mathbf{v}_{r1}=\bar{\gamma}_r\mathbf{v}_{r1} \quad \text{(A5)}$$

Applying (A4) in (A5) leads to

$$\begin{aligned}\mathbf{\Psi}\mathbf{v}_{r1}&=\left(g_r+jh_r\right)\left(\bar{\mathbf{v}}_{r1}+j\tilde{\mathbf{v}}_{r1}\right)=\left(g_r\bar{\mathbf{v}}_{r1}-h_r\tilde{\mathbf{v}}_{r1}\right)+\\&+j\left(g_r\tilde{\mathbf{v}}_{r1}+h_r\bar{\mathbf{v}}_{r1}\right)\end{aligned} \quad \text{(A6)}$$

Eq. (A6) can be divided to following equations

$$\mathbf{\Psi}\bar{\mathbf{v}}_{r1}=g_r\bar{\mathbf{v}}_{r1}-h_r\tilde{\mathbf{v}}_{r1},\quad \mathbf{\Psi}\tilde{\mathbf{v}}_{r1}=g_r\tilde{\mathbf{v}}_{r1}+h_r\bar{\mathbf{v}}_{r1} \quad \text{(A7)}$$

Eq. (A7) is equivalent to

$$\mathbf{\Psi}\begin{bmatrix}\bar{\mathbf{v}}_{r1} & \tilde{\mathbf{v}}_{r1}\end{bmatrix}=\begin{bmatrix}\bar{\mathbf{v}}_{r1} & \tilde{\mathbf{v}}_{r1}\end{bmatrix}\begin{bmatrix}g_r & h_r\\ -h_r & g_r\end{bmatrix}=\begin{bmatrix}\bar{\mathbf{v}}_{r1} & \tilde{\mathbf{v}}_{r1}\end{bmatrix}\bar{\mathbf{\Pi}}_r \quad \text{(A8)}$$

For $1<k\leq n_r$, it can be written that

$$\mathbf{\Psi}\mathbf{v}_{rk}=\bar{\lambda}_r\mathbf{v}_{rk}+\mathbf{v}_{r(k-1)} \quad \text{(A9)}$$

Replacing (A4) in (A9), will result to

$$\begin{aligned}\mathbf{\Psi}\mathbf{v}_{rk}&=\mathbf{\Psi}\left(\bar{\mathbf{v}}_{rk}+j\tilde{\mathbf{v}}_{rk}\right)=\left(g_r\bar{\mathbf{v}}_{rk}-h_r\tilde{\mathbf{v}}_{rk}+\bar{\mathbf{v}}_{r(k-1)}\right)+\\&+j\left(g_r\tilde{\mathbf{v}}_{rk}+h_r\bar{\mathbf{v}}_{rk}+\tilde{\mathbf{v}}_{r(k-1)}\right)\end{aligned} \quad \text{(A10)}$$

In matrix form, (A10) can be written as follows

$$\begin{aligned}&\mathbf{\Psi}\begin{bmatrix}\bar{\mathbf{v}}_{rk} & \tilde{\mathbf{v}}_{rk}\end{bmatrix}=\\&=\begin{bmatrix}\bar{\mathbf{v}}_{r(k-1)} & \tilde{\mathbf{v}}_{r(k-1)} & \bar{\mathbf{v}}_{rk} & \tilde{\mathbf{v}}_{rk}\end{bmatrix}\begin{bmatrix}1 & 0 & g_r & -h_r\\ 0 & 1 & h_r & g_r\end{bmatrix}^T\\&=\begin{bmatrix}\bar{\mathbf{v}}_{r(k-1)} & \tilde{\mathbf{v}}_{r(k-1)} & \bar{\mathbf{v}}_{rk} & \tilde{\mathbf{v}}_{rk}\end{bmatrix}\begin{bmatrix}\mathbf{I}_2 & \bar{\mathbf{\Pi}}_r\end{bmatrix}^T\end{aligned} \quad \text{(A11)}$$

Therefore, for rth eigenvalue with repetition order n_r, the matrix $\mathbf{v}_r$ will be in the following form

$$\mathbf{v}_r=[\bar{\mathbf{v}}_{r1},\tilde{\mathbf{v}}_{r1},\bar{\mathbf{v}}_{r2},\tilde{\mathbf{v}}_{r2},...,\bar{\mathbf{v}}_{rn_r},\tilde{\mathbf{v}}_{rn_r}] \quad \text{(A12)}$$

So that, we can write

$$\mathbf{\Psi v}_r = \mathbf{v}_r \mathbf{\Pi}_r \tag{A13}$$

where $\mathbf{\Pi}_r$ is defined in eq. (10). In continuance of the proof, matrix $\mathbf{V} \in \Re^{N\times N}$ is defined as follows

$$\mathbf{V} = \left[\tilde{\mathbf{V}}_1, ..., \tilde{\mathbf{V}}_n, \mathbf{V}_{n+1}, ..., \mathbf{V}_{n+m} \right] \tag{A14}$$

In (A14), the first n-blocks are corresponding to real eigenvalues and other blocks following (A12) are corresponding to complex eigenvalues. Now we can write that

$$\mathbf{\Psi V} = \mathbf{V \Pi} \tag{A15}$$

Finally, the non-singularity of $\mathbf{V}$ should be proven. For imaginary eigenvalues we can write that

$$\bar{\mathbf{v}}_{rk} = \frac{\mathbf{v}_{rk} + \mathbf{v}_{rk}^*}{2}, \qquad \tilde{\mathbf{v}}_{rk} = \frac{\mathbf{v}_{rk} - \mathbf{v}_{rk}^*}{2} \tag{A16}$$

We define the matrix $\mathbf{\Omega} = \frac{1}{2} diag\{\mathbf{\Omega}_1, \mathbf{\Omega}_2, ..., \mathbf{\Omega}_{n+m}\}$, where

$$\mathbf{\Omega}_i = 2,\ i = 1, 2, ..., n, \quad \mathbf{\Omega}_i = \begin{bmatrix} 1 & 1 \\ 1 & -1 \end{bmatrix} \\ , i = n+1, ..., n+m \tag{A16}$$

Now we can write $\mathbf{V} = \tilde{\mathbf{V}}\mathbf{\Omega}$. Since the matrices $\mathbf{\Omega}$ and $\tilde{\mathbf{V}}$ are non-singular, it is inferred that $\mathbf{V}$ is also non-singular. So that, from (A15), we can write

$$\mathbf{V}^{-1}\mathbf{\Psi V} = \mathbf{\Pi} \tag{A18}$$

and the proof is complete.

7.4. Gresgorin theorem

Let $\mathbf{Q} = [q_{ij}] \in \Re^{N\times N}$ be a square matrix. The all eigenvalues of $\mathbf{Q}$ are located in the union of N disks.

$$\bigcup_{i=1}^{N} \left\{ z \in \Re : \left\| z - q_{ii} \right\| \le \sum_{j=1, \ne i}^{N} \left| q_{ij} \right| \right\} \tag{A19}$$